Biomedical Physics &
Engineering Express

Endorsed by IPEM Institute of Physics and Engineering in Medicine
PURPOSE-LED PUBLISHING™

PAPER

Dosimetric comparison of the anisotropic analytical algorithm and Acuros XB for single-fraction cranial stereotactic radiosurgery with a 6 MV flattening filter-free beam

To cite this article: Kananan Utitsarn *et al* 2026 *Biomed. Phys. Eng. Express* **12** 055048

View the article online for updates and enhancements.

You may also like

- Influence of multiple brain metastases' size and number on the quality of SRS – VMAT dose delivery
G Prentou, E Koutsouveli, E Pantelis et al.
- Dosimetric comparison between single and double isocenters VMAT for SRT with multiple targets
Wai Lwin Lwin Kyaw, Sivalee Suriyapee, Chotika Jumpangern et al.
- Robust and optimal dose distribution for brain metastases with robotic radiosurgery system: recipe for an inflection point
Ryoichi Hinoto, Nobuhiro Tsukamoto, Takahisa Eriguchi et al.

This content was downloaded from IP address 202.28.152.231 on 14/10/2026 at 07:57

Biomedical Physics & Engineering Express

Check for updates

PAPER

RECEIVED
18 June 2026

REVISED
22 September 2026

ACCEPTED FOR PUBLICATION
6 October 2026

PUBLISHED
14 October 2026

Dosimetric comparison of the anisotropic analytical algorithm and Acuros XB for single-fraction cranial stereotactic radiosurgery with a 6 MV flattening filter-free beam

Kananan Utitsarn*, Thepphithak Watthanasarn, Wirasinee Chaloemchawalit and Komkrit Krongkietlearts

Department of Radiotherapy, Lopburi Cancer Hospital, Lopburi, Thailand
* Author to whom any correspondence should be addressed.

E-mail: kananmim@hotmail.com

Keywords: stereotactic radiosurgery, Acuros XB, anisotropic analytical algorithm, dose calculation, EPID dosimetry, brain metastases, flattening filter-free

Supplementary material for this article is available online

Abstract

Stereotactic radiosurgery delivers an ablative single-fraction dose to small intracranial targets, and the reported dose depends on the calculation algorithm. This exploratory case series quantified the change in reported dosimetry when plans clinically finalised with the anisotropic analytical algorithm (AAA) were recalculated with Acuros XB (AXB) in dose-to-medium mode. Seven consecutive brain metastases in six patients, treated with 6 MV flattening filter-free volumetric modulated arc therapy, were recalculated on the same CT dataset using identical arc geometry, control points, multileaf collimator sequences and monitor units, without re-optimisation or renormalisation. Dose-volume histogram parameters were compared for the planning target volume (PTV), normal brain and organs at risk, and plan quality with the RTOG prescription-isodose-to-target-volume (PITV) ratio, the Paddick conformity index (PCI) and the gradient index (GI). Paired comparisons used exact two-sided Wilcoxon signed-rank tests and are interpreted as exploratory. AXB reported lower PTV dose metrics than AAA for the same deliverable plans, with mean D95% falling from 21.66 to 21.10 Gy, D98% from 21.19 to 20.58 Gy and Dmean from 24.58 to 24.13 Gy (all $p = 0.016$). The mean paired D98% difference was $3.00 \pm 0.80\%$ of the prescription dose. The PITV ratio fell from 1.19 to 1.10 and GI rose from 3.23 to 3.43 (both $p = 0.016$), whereas PCI did not differ (0.79 versus 0.82, $p = 0.188$). Normal-brain V12Gy and V10Gy were unchanged. Routine electronic portal imaging device dosimetry of the delivered plans gave a mean 2%/2 mm gamma passing rate of $98.5 \pm 1.7\%$, documenting deliverability rather than validating either algorithm. These findings support careful review of target-dose metrics when an established AAA workflow is transitioned to AXB. The cohort is small and no independent reference dosimetry was available, so the study establishes neither clinical superiority nor an effect on tumour control or toxicity.

1. Introduction

Stereotactic radiosurgery (SRS) uses highly conformal beams to deliver an ablative dose to small intracranial targets with steep dose gradients. Accurate target definition, treatment planning, and delivery are therefore essential. The accuracy and reported characteristics of an SRS dose distribution depend on more than the patient dose-calculation algorithm alone; relevant factors include treatment-planning-system commissioning and small-field beam data, computed tomography (CT) image quality and CT-to-density/material calibration, dose-grid resolution, CT slice thickness, target delineation, and geometric accuracy across the stereotactic workflow (Das *et al* 2008, Cirino 2025, Rojas-López *et al* 2025, Soares *et al* 2026).

AAA and Acuros XB (AXB) are available in the Varian Eclipse treatment planning system (TPS). AAA is a convolution/superposition algorithm that

© 2026 IOP Publishing Ltd. All rights, including for text and data mining, AI training, and similar technologies, are reserved.

uses density-scaled kernels, whereas AXB deterministically solves the linear Boltzmann transport equation (Ulmer *et al* 2005, Vassiliev *et al* 2010). AXB has shown closer agreement than AAA with Monte Carlo calculations in heterogeneous media (Bush *et al* 2011). Intracranial targets are usually embedded in relatively homogeneous brain parenchyma, but SRS still involves small fields, steep gradients, skull and air interfaces, and potentially very small targets, all of which can increase sensitivity to calculation and spatial-resolution choices.

Previous work has already demonstrated algorithm-dependent differences in radiosurgery. One study recalculated 20 AAA-based RapidArc plans for solitary brain metastases with AXB while keeping arc orientations, multileaf collimator (MLC) apertures, and monitor units unchanged, and included independent phantom measurements (Menon *et al* 2022). A second study showed that calculation-algorithm class, target size, lesion number, and fractionation can influence multiple SRS quality indices (Rojas-López *et al* 2024), while a third quantified the sensitivity of cranial dose metrics to calculation-grid resolution (Soares *et al* 2026). The present study therefore does not aim to establish the general superiority of a type-C algorithm. Instead, it examines a practical clinical transition scenario: 6 MV flattening filter-free (FFF) SRS plans clinically finalised with AAA were recalculated with AXB dose-to-medium while preserving all deliverable treatment parameters, and changes in target dose, normal-brain dose, SRS-specific conformity and gradient metrics, target-size and bone-proximity associations, and the context of routine institutional patient-specific quality assurance (PSQA) were characterised.

2. Methods

2.1. Patient cohort

Seven brain metastases in six patients treated with single-fraction SRS at a single institution between 2025 and 2026 were included (table 1). One patient had two metastases, each planned and treated separately; consequently, this cohort did not include nearby targets within a common plan or dose-bridging between lesions. The cohort was analysed as an exploratory lesion-level case series. Prescription doses ranged from 15 to 24 Gy and were selected clinically according to lesion size, prior treatment, and normal-tissue and organ-at-risk considerations. Case 2 had previously received whole-brain radiotherapy, and the 15 Gy single-fraction prescription was an individualised re-irradiation decision rather than one taken against the size-based thresholds in current guidance (Shaw *et al* 2000, Gondi *et al* 2022). The measured maximum planning target volume (PTV) diameter of 2.74 cm is reported as a planning-structure descriptor and is not used as a surrogate for gross-lesion diameter in size-based treatment guidelines. This case is reported as it was treated and is not offered as a dose recommendation. The study was approved by the institutional review board on 11 February 2026 (approval number REC002/69) and was conducted in accordance with the Declaration of Helsinki. Because the analysis was retrospective and used only existing treatment planning data, the requirement for individual informed consent was waived by the approving committee.

2.2. TPS and linear accelerator

All treatment plans were created using Eclipse version 17.01 and delivered on a TrueBeam linear accelerator (Varian Medical Systems, Palo Alto, CA, USA) using 6 MV FFF beams and non-coplanar volumetric modulated arc therapy (VMAT). Planning CT images were acquired with 1 mm slice thickness on an Aquilion ONE scanner (Canon Medical Systems Corporation, Otawara, Tochigi, Japan). Patients were immobilised with the Encompass SRS Immobilization System (Qfix, Avondale, PA, USA). A 1.25 mm final dose-calculation grid was used for both AAA and AXB because this was the clinically commissioned high-resolution SRS setting during the study period. When the workflow was established, graphics processing unit accelerated dose calculation was not available, and 1.25 mm was selected as a practical balance between spatial resolution and calculation time. Current AAPM-RSS Medical Physics Practice Guideline 9.b recommends an isotropic grid of 2 mm or finer and notes that a 1 mm grid may be necessary for very small targets ($\leqslant 1$ cm^3) or targets adjacent to critical organs at risk (OARs) (Cirino 2025). A dedicated 1.0 mm sensitivity analysis was not available for this retrospective cohort, and the consequences for the smallest lesions are considered in section 5.

2.3. SRS-relevant beam commissioning

Only the clinically relevant 6 MV FFF beam-model context is summarised. Percentage depth doses and profiles used for commissioning extended to 2×2 cm^2 and were measured with a microDiamond detector (type 60019, PTW, Freiburg, Germany). Small-field output factors entered into the TPS were corrected according to the IAEA-AAPM TRS-483 formalism (IAEA 2017). Additional measurements were acquired down to 1×1 cm^2 using the microDiamond detector, an EDGE diode detector (Sun Nuclear, Melbourne, FL, USA), and an Exradin W2 scintillation detector (Standard Imaging, Middleton, WI, USA) as cross-detector small-field checks. These 1×1 cm^2 measurements were not direct beam-model inputs and are not presented as a formal calculated-versus-measured 1×1 cm^2 TPS validation.

Table 1. Lesion and treatment characteristics ($n = 7$). Minimum PTV-to-bone distance is a signed in-plane edge-to-edge distance measured on the planning CT; negative values indicate overlap of the PTV with the radiation-oncologist-contoured bone structure. VMAT, volumetric modulated arc therapy.

Case	PTV volume (cm^3)	Maximum PTVdiameter (cm)	Minimum in-plane PTV-to-bone distance (cm)	Prescribed dose (Gy)	VMAT arcs
1	2.3	2.53	0.78	20	4
2	9.7	2.74	0.66	15	6
3	1.2	1.26	0.38	20	4
4	0.9	1.81	2.07	24	3
5	0.7	1.36	0.44	20	5
6	1.5	1.45	−0.22	24	4
7	0.9	1.24	0.47	20	4

2.4. Treatment planning methodology

VMAT plans were optimised using the institutional Eclipse workflow and clinically finalised with AAA because AAA was the established calculation method during the study period; AAA was used as the clinical baseline and not as a dosimetric reference standard. After physician approval, each plan was recalculated with AXB using the same patient CT dataset, structure set, arc geometry, control points/MLC sequences, and monitor units, without re-optimisation or renormalisation. AXB was evaluated in dose-to-medium (Dm,m) reporting mode. AAA has a single dose-reporting convention based on density-scaled water kernels, whereas AXB Dm,m reports absorbed dose to the local medium; consequently, the comparison combines differences in radiation-transport modelling and dose-reporting convention rather than isolating either effect (Andreo 2015, Gopalakrishnan *et al* 2022). Each plan used three to six non-coplanar VMAT arcs.

2.5. Dose-volume histogram (DVH) analysis

DVH parameters were extracted from Eclipse for both calculations. For the PTV, D95%, D98%, and Dmean were evaluated in Gy. Because prescriptions varied from 15 to 24 Gy, the lesion-level D98% difference was additionally normalised to the prescription dose of that lesion as shown in equation (1), and the normalised difference ΔD98Rx was used for the exploratory anatomical association analyses.

$$\Delta\mathrm{D98Rx}\,(\%) = 100 \times (\mathrm{D98\%AAA} - \mathrm{D98\%AXB}) \,/\,\text{prescribed dose}. \quad (1)$$

Normal brain was defined as whole brain minus gross tumour volume (Brain − GTV), consistent with published single-fraction SRS dose-volume analyses (Milano *et al* 2021). V12Gy was treated as the principal normal-brain dose-volume metric because of its established association with radiation necrosis after SRS; V10Gy and V6Gy were retained as exploratory descriptors of intermediate- and lower-dose spill (Milano *et al* 2021).

OARs evaluated were the brainstem, ipsilateral optic nerve, optic chiasm, and lens. Near-maximum dose (D0.03 cm^3) was recorded for the brainstem, optic nerve, and optic chiasm, and Dmax for the lens. OARs not contoured for a given lesion were excluded from that comparison. For the anatomical sensitivity analysis, the nearest bony structure was manually contoured by the radiation oncologist on the planning CT. The minimum in-plane edge-to-edge distance from PTV to the bone contour was measured on the CT slice showing the closest approach; positive values indicate separation and negative values indicate overlap.

2.6. Plan quality indices

The RTOG prescription-isodose-to-target-volume (PITV) ratio was retained as a secondary conformity descriptor for comparison with prior literature (Shaw *et al* 1993) and is defined in equation (2).

$$\text{RTOG PITV ratio} = \mathrm{PIV100\%/TV} \quad (2)$$

where PIV100% is the volume enclosed by the prescription isodose surface and TV is the target volume. A ratio below 1 necessarily implies incomplete prescription-isodose coverage of the target, whereas a value above 1 may reflect dose spill outside the target but does not by itself establish adequate target coverage. Because the PITV ratio does not jointly account for target coverage and selectivity, the Paddick conformity index (PCI) was added as the preferred conformity metric (Paddick 2000) and is defined in equation (3).

$$\mathrm{PCI} = (\mathrm{TVPIV})^2 / (\mathrm{TV} \times \mathrm{PIV100\%}) \quad (3)$$

where TVPIV is the portion of the target covered by the prescription isodose. PCI ranges from 0 to 1, with 1 representing complete target coverage without prescription-dose spill outside the target.

Dose fall-off was assessed using the Paddick gradient index (GI) (Paddick and Lippitz 2006), which is defined in equation (4).

$$\mathrm{GI} = \mathrm{PIV50\%/PIV100\%} \quad (4)$$

where PIV50% is the volume enclosed by the 50% prescription isodose surface. A lower GI indicates a

steeper calculated dose fall-off. Because the plans were not re-optimised or renormalised after AXB recalculation, changes in the PITV ratio or GI are interpreted as changes in dosimetric characterisation of the same delivery rather than as changes in physical plan quality.

2.7. Plan verification

Routine PSQA was performed for each clinically approved treatment plan using portal dosimetry on the TrueBeam aS1200 electronic portal imaging device (EPID). A verification plan was created after physician approval; gantry and collimator angles were retained, and for non-coplanar arcs the couch angle was reset to 0° for EPID acquisition. Eclipse portal dose image prediction (PDIP) generates an EPID-specific predicted portal image from treatment-delivery information and an EPID-response model; it is not a direct measurement or reconstruction of the three-dimensional patient dose calculated with AAA or AXB (Dogan *et al* 2023, Calvo-Ortega 2024). Accordingly, the revised PSQA analysis is used only to document deliverability of the clinically approved treatment sequences and not to compare the intrinsic patient-dose accuracy of AAA and AXB. Gamma analysis used the institutional 2%/2 mm global criterion, global normalisation to the maximum dose, a 10% low-dose threshold, and a $\geqslant$95% acceptance level. The gamma passing rate reported for each lesion is the composite value for all arcs of that plan and is not the average of the individual per-arc values. AAPM Task Group 218 recommends 3%/2 mm with a 10% threshold as a general intensity-modulated radiotherapy (IMRT) and VMAT benchmark and notes that tighter criteria may be appropriate for stereotactic treatments; the institutional protocol used a tighter 2% dose-difference criterion while retaining 2 mm distance-to-agreement (Miften *et al* 2018). A prospectively defined 1 mm gamma analysis was not part of the original clinical protocol. Because the couch was reset to 0° for EPID acquisition, this pretreatment PSQA did not test non-coplanar couch-angle positioning, patient setup, or rotational treatment accuracy. No independent film/detector-array measurement was performed specifically for these seven SRS cases (Dogan *et al* 2023).

2.8. Statistical analysis

Paired differences between AAA and AXB for DVH parameters and plan-quality indices were evaluated using exact two-sided Wilcoxon signed-rank tests because only seven lesion-level pairs were available. No correction for multiple comparisons was applied; individual p values are therefore interpreted as exploratory rather than confirmatory. For metrics with seven non-zero paired differences, $p = 0.015625$ is the minimum attainable two-sided exact Wilcoxon p value and is reported as $p = 0.016$. Statistical calculations were performed in Python using SciPy (Virtanen *et al* 2020). Associations of ΔD98Rx with PTV volume, maximum PTV diameter, and minimum in-plane PTV-to-bone distance were evaluated using Spearman rank correlations with exact permutation p values. The lesion was the unit of analysis. Because two lesions arose in one patient, complete statistical independence between all seven lesion-level observations cannot be assumed.

3. Results

3.1. Dosimetric comparison

AXB reported lower PTV dose metrics than AAA for the same deliverable plans. D95% decreased from 21.66 to 21.10 Gy, D98% from 21.19 to 20.58 Gy, and Dmean from 24.58 to 24.13 Gy (all $p = 0.016$). The mean paired D98% reduction was 0.61 Gy and corresponded to 3.00 $\pm$ 0.80% of the prescription dose across the seven lesions (median 3.17%; range 1.85–3.95%). Paired differences for D98%, D95%, and Dmean in each lesion are given in supplementary tables S1 to S3, respectively.

The RTOG PITV ratio was lower with AXB (1.10 ± 0.18) than with AAA (1.19 ± 0.17; $p = 0.016$). In contrast, PCI was 0.79 $\pm$ 0.10 for AAA and 0.82 $\pm$ 0.12 for AXB and did not differ significantly ($p = 0.188$). GI increased from 3.23 $\pm$ 0.59 with AAA to 3.43 $\pm$ 0.63 with AXB ($p = 0.016$). Because the delivery parameters were unchanged and the AXB dose distribution was not renormalised, the lower PITV ratio and higher GI describe how fixed prescription-isodose surfaces changed under recalculation and should not be interpreted as a demonstrated improvement or deterioration in physical plan quality.

For Brain − GTV, V12Gy and V10Gy did not differ significantly between algorithms ($p = 0.156$ for both). V6Gy was lower with AXB, 19.16 versus 19.90 cm^3 ($p = 0.016$), and is interpreted as an exploratory lower-dose-spill difference rather than a clinical outcome endpoint.

Among OARs, optic-chiasm D0.03 cm^3 was lower with AXB, 0.55 versus 0.66 Gy ($p = 0.031$). Brainstem, optic nerve, and lens doses were not significantly different ($p = 0.313$, 0.094, and 0.188, respectively). No inference regarding toxicity or clinical outcome was made from these low absolute OAR doses.

Exploratory anatomical analyses did not identify a statistically significant predictor of ΔD98Rx. The Spearman correlation was $\rho = -0.631$ for PTV volume (exact $p = 0.143$), $\rho = -0.214$ for maximum PTV diameter ($p = 0.662$), and $\rho = 0.321$ for minimum in-plane PTV-to-bone distance ($p = 0.498$). Case 6 had a negative PTV-to-bone distance (−0.22 cm), indicating overlap with the contoured bone structure, but did not show the largest D98%

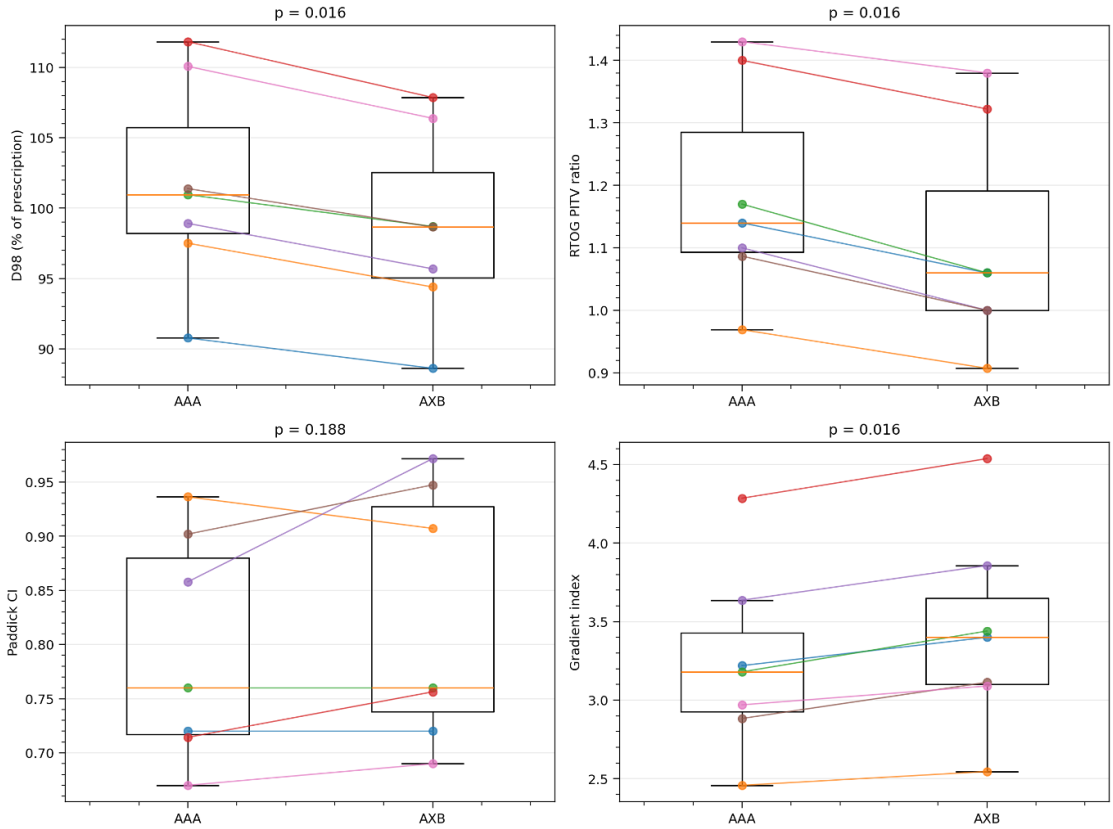


Figure 1. Lesion-level paired comparison of AAA and AXB for PTV D98% normalised to prescription dose, RTOG PITV ratio, Paddick conformity index, and gradient index. Box plots show the cohort distribution and connected points show paired values for each lesion ($n = 7$). p values are from exact two-sided Wilcoxon signed-rank tests. D98% is shown as a percentage of prescription; the conformity and gradient indices are dimensionless.

Table 2. PTV dose and plan-quality metrics for AAA and AXB ($n = 7$). Values are mean ± standard deviation (SD). p values are from two-sided Wilcoxon signed-rank tests and are interpreted as exploratory.

Metric	AAA	AXB	p
D95% (Gy)	21.66 ± 3.87	21.10 ± 3.77	0.016
D98% (Gy)	21.19 ± 3.85	20.58 ± 3.71	0.016
Dmean (Gy)	24.58 ± 3.88	24.13 ± 3.84	0.016
RTOG PITV ratio	1.19 ± 0.17	1.10 ± 0.18	0.016
PCI	0.79 ± 0.10	0.82 ± 0.12	0.188
GI	3.23 ± 0.59	3.43 ± 0.63	0.016

Table 3. Normal brain dose-volume metrics for AAA and AXB ($n = 7$). Values are mean ± SD in cm^3.

Metric	AAA	AXB	p
V12Gy (cm^3)	5.06 ± 2.89	4.96 ± 2.77	0.156
V10Gy (cm^3)	7.64 ± 5.33	7.52 ± 5.20	0.156
V6Gy (cm^3)	19.90 ± 18.06	19.16 ± 17.02	0.016

Table 4. Organ-at-risk doses for AAA and AXB. Values are mean ± SD in Gy. n is the number of lesions for which the structure was contoured, so it is the number of paired observations entering each test rather than the number of patients.

OAR	Metric	n	AAA	AXB	p
Brainstem	D0.03 cm^3	6	1.08 ± 0.84	1.03 ± 0.85	0.313
Optic nerve	D0.03 cm^3	6	0.94 ± 1.12	0.89 ± 1.11	0.094
Optic chiasm	D0.03 cm^3	6	0.66 ± 0.50	0.55 ± 0.46	0.031
Lens	Dmax	5	0.34 ± 0.29	0.32 ± 0.28	0.188

Table 5. Routine patient-specific EPID gamma passing rates for the seven AAA-finalised clinically delivered plans, composite for all arcs of each plan, using the institutional 2%/2 mm global criterion and a 10% low-dose threshold.

Case	Prescribed dose (Gy)	Gamma passingrate (%)
1	20	97.5
2	15	97.0
3	20	99.0
4	24	100.0
5	20	100.0
6	24	100.0
7	20	95.9
Mean ± SD		98.5 ± 1.7

difference. These data do not support bone proximity as the primary explanation for the observed AAA − AXB difference in this cohort.

3.2. Routine patient-specific QA

Routine EPID-based PSQA of the seven clinically delivered plans yielded a mean 2%/2 mm gamma passing rate of 98.5 ± 1.7% (range 95.9–100.0%). All seven plans met the institutional ⩾95% acceptance level. These data document deliverability within the institutional portal-dosimetry workflow and are not used as an AAA-versus-AXB dose-accuracy comparison.

4. Discussion

The central finding of this exploratory clinical case series is that AXB dose-to-medium reported systematically lower PTV dose metrics than the institutional AAA calculation when the same deliverable SRS plans were recalculated without re-optimisation or renormalisation. The mean D98% difference was 0.61 Gy, corresponding to 3.00% of prescription. This should be interpreted as an algorithm- and reporting-dependent change in the dosimetric characterisation of a fixed delivery, not as direct evidence that the AAA-based clinical plan physically delivered an incorrect dose. AAA and AXB differ in radiation-transport modelling, and the present comparison also contrasts AAA's single water-kernel-based reporting convention with AXB dose-to-medium. The study design therefore cannot assign the observed difference uniquely to transport modelling or dose-reporting convention.

The direction of the target-dose differences is consistent with prior literature, but the contribution of the present study is incremental rather than a first demonstration of type-B versus type-C behaviour. An earlier study evaluated 20 solitary brain-metastasis RapidArc plans recalculated with AXB using unchanged delivery parameters and additionally performed ion-chamber, optically stimulated luminescence dosimeter, and EPID validation (Menon *et al* 2022). The present work contributes institution-specific data from a contemporary 6 MV FFF TrueBeam workflow using AXB dose-to-medium, adds PCI and quantitative target-size/bone-distance analyses, and explicitly separates routine EPID deliverability QA from validation of patient-dose algorithm accuracy. Recent cranial radiosurgery studies using Monte Carlo or other type-C methods further show that small targets, multiple-target geometry, and grid resolution can materially influence reported plan-quality metrics (Rojas-López *et al* 2024, Soares *et al* 2026). The current results should therefore be viewed as exploratory clinical implementation evidence rather than broadly generalisable proof of algorithm superiority.

Three features of the design support the internal validity of these comparisons at this cohort size. The series is consecutive and covers every SRS case treated in the period, so no case selection was applied. Each lesion also serves as its own control, since the two calculations share the patient anatomy, the arc geometry, the MLC sequence and the monitor units, and neither re-optimisation nor renormalisation intervened, so the calculation is what differs between the paired values. The paired D98% difference was negative in seven of seven lesions, and the consistency of that direction, rather than the size of any individual difference, is what a paired design at this cohort size is able to establish. The anatomical associations were reported whether or not they reached significance, and none of the three did. For a department moving an established AAA workflow to AXB, the practical value of these data is the magnitude to expect, a mean D98% reduction of 3.00% of the prescription dose, together with the observation that the direction did not vary across the series.

The plan-quality results also illustrate why the RTOG conformity ratio should not be interpreted in isolation. Although the RTOG ratio decreased significantly with AXB, PCI—which incorporates both target coverage and selectivity—did not differ significantly. GI increased with AXB. Because the MLC sequences, monitor units, control points, and beam geometry were unchanged and no renormalisation was performed, these index changes reflect movement of fixed isodose surfaces under the alternative dose-calculation/reporting method rather than a change in the deliverable beam parameters or a demonstrated improvement in plan quality. The absence of a significant PCI difference therefore argues against describing AXB as producing 'tighter conformity' in these unchanged plans.

For normal brain, V12Gy—the most clinically established single-fraction SRS brain dose-volume metric—did not differ significantly between calculations, nor did V10Gy. The mean V6Gy difference was 0.74 cm^3 and is best regarded as an exploratory lower-dose-spill finding rather than

a clinical-outcome endpoint. The optic-chiasm D0.03 cm^3 difference was also statistically significant, but the absolute doses were low in this cohort and no clinical-outcome inference can be made. The study was not designed to assess toxicity or local control.

Portal dosimetry must be interpreted separately from the patient-dose comparison. PDIP predicts EPID detector response using treatment-delivery information and a detector-response model rather than independently measuring the three-dimensional AAA or AXB patient dose (Dogan *et al* 2023, Calvo-Ortega 2024). All clinically delivered plans met the institutional 2%/2 mm PSQA criterion, supporting deliverability of the treatment sequences used in this cohort. However, the couch angle was reset to 0° for EPID acquisition, so this PSQA did not evaluate non-coplanar couch-angle positioning or patient translational/rotational setup accuracy. No film or detector-array measurement was performed specifically for these seven SRS cases, and no independent reference dosimetry was included in the present study. Portal dosimetry therefore cannot be used here to establish that one patient-dose algorithm is more accurate than the other.

The quantitative size and bone-proximity analyses also modify the mechanistic interpretation of the original manuscript. Smaller PTVs showed only a non-significant trend toward a larger prescription-normalised D98% difference, and maximum PTV diameter was not associated with the difference. Minimum in-plane PTV-to-bone distance was likewise not significantly associated with the D98% difference. One target overlapped the contoured bone structure, yet it did not have the largest algorithm-dependent dose difference. The present data therefore do not support the previous causal statement that skull proximity accounts for the systematic AAA − AXB difference. More detailed studies using three-dimensional distance maps, deliberately selected bone/air-interface cases, and independent reference dosimetry would be required to test that mechanism.

5. Limitations

This study has several limitations. First, the cohort comprised only seven lesions in six patients, which limits precision, prevents population-level generalisation, and makes all significance tests exploratory; two lesions arose in one patient, so lesion-level observations may not be completely independent. Second, the cohort did not include nearby targets within a common plan and therefore cannot address dose bridging in multiple-metastasis SRS. Third, the clinical 1.25 mm calculation grid was retained; current guidance notes that a 1 mm grid may be necessary for very small targets, and no dedicated 1.0 mm sensitivity analysis was available for this cohort (Cirino 2025, Soares *et al* 2026). The study also does not present a formal calculated-versus-measured 1 × 1 cm^2 TPS validation dataset, although cross-detector measurements were available at that field size. Fourth, AXB was evaluated only in dose-to-medium mode, so the effects of changing the transport algorithm and reporting convention cannot be disentangled. Fifth, PTV-to-bone distance was measured in-plane on CT rather than with a three-dimensional distance-map method. Sixth, PSQA used linac-integrated EPID portal dosimetry; a 1 mm gamma analysis was not part of the original protocol, the couch reset prevented evaluation of non-coplanar couch-angle accuracy, and no independent film/detector-array measurement or independent reference-dose calculation was included. Finally, the study is single-institutional and represents a specific Eclipse/TrueBeam/6 MV FFF workflow. Larger multi-institutional datasets with deliberately challenging small-target, bone/air-interface, and multiple-target geometries, together with independent reference dosimetry, are needed.

6. Conclusion

In this exploratory clinical case series, recalculation of clinical single-fraction SRS plans finalised with AAA using AXB dose-to-medium changed the reported target-dose and plan-quality metrics despite identical deliverable beam parameters. The mean D98% difference was approximately 3% of prescription, while PCI did not show a significant algorithm-dependent difference.

Routine EPID-based PSQA confirmed that all clinically delivered plans met the institutional 2%/2 mm acceptance criterion, but portal dosimetry was not used as an independent comparison of AAA and AXB patient-dose accuracy.

The findings support careful review of target-dose metrics when an established AAA SRS workflow is transitioned to AXB, including in relatively homogeneous intracranial anatomy. However, the limitations set out in section 5 preclude claims of clinical superiority or outcome benefit. Larger studies incorporating deliberately challenging small-target and interface geometries, multiple-target scenarios, finer-grid sensitivity analyses, and independent reference dosimetry are warranted.

Acknowledgment

This research received no external funding. Generative AI tools were used during manuscript preparation: Claude Opus 4.8 (Anthropic, San Francisco, CA, USA) and ChatGPT (GPT-5.6 Sol; OpenAI, San Francisco, CA, USA) were used for language editing, structural revision, and

literature-search assistance. No generative AI tool generated or altered the original research data. All scientific content, interpretation, and final decisions remain the responsibility of the authors.

Data availability statement

The aggregated data supporting the findings of this study are presented within the article in tables 2–5 and figure 1. The underlying patient treatment planning data are not publicly available due to patient privacy and institutional ethics restrictions. Anonymised numerical data may be available from the corresponding author upon reasonable request and subject to institutional ethics approval.

Lesion-level dose differences available at: https://doi.org/10.1088/2057-1976/aeb0b1/data1.

Conflict of interest

There are no conflicts of interest.

Author contributions

Kananan Utitsarn 0009-0002-2769-3241
Conceptualization (equal), Data curation (equal), Formal analysis (equal), Investigation (equal), Methodology (equal), Writing – original draft (lead), Writing – review & editing (equal)

Thepphithak Watthanasarn
Data curation (equal), Methodology (equal)

Wirasinee Chaloemchawalit
Data curation (equal), Methodology (equal)

Komkrit Krongkietlearts
Conceptualization (equal), Formal analysis (equal), Methodology (equal), Software (equal), Supervision (equal), Writing – review & editing (equal)

References

Andreo P 2015 Dose to 'water-like' media or dose to tissue in MV photons radiotherapy treatment planning: still a matter of debate *Phys. Med. Biol.* **60** 309–37

Bush K *et al* 2011 Dosimetric validation of Acuros XB with Monte Carlo methods for photon dose calculations *Med. Phys.* **38** 2208–21

Calvo-Ortega J-F 2024 Optimization of a commercial portal dose image prediction algorithm for pre-treatment verifications of plans using unflattened photon beams *Rep. Pract. Oncol. Radiother.* **29** 62–68

Cirino E 2025 AAPM-RSS medical physics practice guideline 9.b: SRS-SBRT *J. Appl. Clin. Med. Phys.* **26** e14624

Das I J *et al* 2008 Accelerator beam data commissioning equipment and procedures: report of the AAPM Task Group 106 *Med. Phys.* **35** 4186–215

Dogan N *et al* 2023 AAPM Task Group Report 307: use of EPIDs for patient-specific IMRT and VMAT QA *Med. Phys.* **50** e865–e903

Gondi V *et al* 2022 Radiation therapy for brain metastases: an ASTRO clinical practice guideline *Pract. Radiat. Oncol.* **12** 265–82

Gopalakrishnan Z *et al* 2022 Dosimetric comparison of analytical anisotropic algorithm and the two dose reporting modes of Acuros XB dose calculation algorithm in volumetric modulated arc therapy of carcinoma lung and carcinoma prostate *Med. Dosim.* **47** 280–7

IAEA 2017 Dosimetry of small static fields used in external beam radiotherapy: an international code of practice for reference and relative dose determination *Technical Reports Series No.* 483 (International Atomic Energy Agency)

Menon S V *et al* 2022 Dosimetric comparison and validation of Eclipse AAA and AcurosXB algorithms in RapidArc-based radiosurgery plans of patients with solitary brain metastasis *Med. Dosim.* **47** e7–e12

Miften M *et al* 2018 Tolerance limits and methodologies for IMRT measurement-based verification QA: recommendations of AAPM Task Group No. 218 *Med. Phys.* **45** e53–e83

Milano M T *et al* 2021 Single- and multifraction stereotactic radiosurgery dose/volume tolerances of the brain *Int. J. Radiat. Oncol. Biol. Phys.* **110** 68–86

Paddick I 2000 A simple scoring ratio to index the conformity of radiosurgical treatment plans *J. Neurosurg.* **93** 219–22

Paddick I and Lippitz B 2006 A simple dose gradient measurement tool to complement the conformity index *J. Neurosurg.* **105** 194–201

Rojas-López J A *et al* 2024 Well calculated is better than quickly calculated: comparison of Pencil beam and Monte Carlo algorithms according to the number of lesions and fractionation in radiosurgery of multiple brain metastases *Phys. Med.* **126** 104827

Rojas-López J A *et al* 2025 Optimizing anisotropic margins in single-isocenter multiple brain metastases radiosurgery using regressor strategies: a multi-institutional validation study *J. Appl. Clin. Med. Phys.* **26** e70249

Shaw E, Kline R, Gillin M, Souhami L, Hirschfeld A, Dinapoli R and Martin L 1993 Radiation Therapy Oncology Group: radiosurgery quality assurance guidelines *Int. J. Radiat. Oncol. Biol. Phys.* **27** 1231–9

Shaw E, Scott C, Souhami L, Dinapoli R, Kline R, Loeffler J and Farnan N 2000 Single dose radiosurgical treatment of recurrent previously irradiated primary brain tumors and brain metastases: final report of RTOG protocol 90–05 *Int. J. Radiat. Oncol. Biol. Phys.* **47** 291–8

Soares N M *et al* 2026 Impact of grid size on dose calculations for cranial tumors *J. Med. Phys.* **51** 277–84

Ulmer W, Pyyry J and Kaissl W 2005 A 3D photon superposition/convolution algorithm and its foundation on results of Monte Carlo calculations *Phys. Med. Biol.* **50** 1767–90

Vassiliev O N *et al* 2010 Validation of a new grid-based Boltzmann equation solver for dose calculation in radiotherapy with photon beams *Phys. Med. Biol.* **55** 581–98

Virtanen P *et al* 2020 SciPy 1.0: fundamental algorithms for scientific computing in Python *Nat. Methods* **17** 261–72